Intelligence & Robotics

Research Article

Networked scheduling for decentralized load frequency control

Chen Peng[1], Hongchenyu Yang[1]

[1]School of Mechatronic Engineering and Automation, Shanghai University, Shanghai 200444, China.

Correspondence to: Prof. Chen Peng, School of Mechatronic Engineering and Automation, Shanghai University, No. 99, Shangda Road, Baoshan District, Shanghai 200444, China. E-mail: c.peng@shu.edu.cn

Abstract

This paper investigates the scheduling process for multi-area interconnected power systems under the shared but band-limited network and decentralized load frequency controllers. To cope with sub-area information and avoid node collision of large-scale power systems, round-robin and try-once-discard scheduling are used to schedule sampling data among different sub-grids. Different from existing decentralized load frequency control methods, this paper studies multi-packet transmission schemes and introduces scheduling protocols to deal with the multi-node collision. Considering the scheduling process and decentralized load frequency controllers, an impulsive power system closed-loop model is well established. Furthermore, sufficient stabilization criteria are derived to obtain decentralized H_∞ output feedback controller gains and scheduling protocol parameters. Under the designed decentralized output feedback controllers, the prescribed system performances are achieved. Finally, a three-area power system example is used to verify the effectiveness of the proposed scheduling method.

Keywords: Multi-area power systems, round-robin scheduling, try-once-discard scheduling, load frequency control

1. INTRODUCTION

With the vigorous development of power markets, the degree of interconnection among power grid regions is increasing. At present, power grids have developed into multi-area interconnected power systems[1,2]. Generally, there are two communication schemes to transmit data between neighborhood areas, that is, the dedicated channel and the open infrastructure. Since the latter has outstanding advantages over the former, such

as higher flexibility and lower cost, it has been widely used in the communication of multi-area interconnected power systems[3–5].

An important indicator to measure power system operation quality is the fluctuation in frequency, and load frequency control (LFC) is widely used to maintain frequency interchanges at scheduled values and stifle frequency fluctuation caused by load disturbances[2,6,7]. Under the open communication infrastructure, the sensor in each area collects data information. Then, data is transmitted to the decentralized controller under the shared but band-limited network. The corresponding control commands are issued to actuators in each area respectively. However, due to the introduction of the network, the design and operation of LFC face some new challenges, such as node collision, data loss and network-induced delay[8–10].

Due to different locations of sub-region power grids and the wide distribution of system components, multi-channel transmission is inevitable in multi-area interconnected power systems, while most of the existing results[10–13] take the general assumption that sampled data is packaged into a single packet to transmit, which is not applied in large-scale multi-area interconnected power systems. On the other hand, the shared network has limited bandwidth, where the simultaneous transmission under multiple channels may cause node congestion. To solve this problem, scheduling protocols have been presented to decide which node to gain access to the communication network[15?].

Generally, multi-channel scheduling includes Round-Robin (RR) scheduling[16,17], try-once-discard (TOD) scheduling[18,19], and stochastic scheduling[20]. Under the RR scheduling protocol, each node is transmitted periodically with a fixed period whose value is the total number of transmission channels. Under the TOD scheduling, the sensor node with the largest scheduling error has access to the channel. Recently, a time-delay analysis method has been discussed to derive stability criteria for networked control systems (NCSs) which are scheduled by the above three communication protocols[14,21]. Besides, a hybrid system method has been employed to analyze NCSs with variable delays under the TOD communication protocol[19], where a partial exponential stabilization criterion has been derived. The H_∞ filtering of NCSs with multiple nodes has been investigated[22], in which TOD protocol is used to schedule sampled data.

This paper studies the H_∞ LFC for multi-area interconnected power systems with decentralized controllers under the shared but band-limited network. RR and TOD protocols are used to schedule the sampling information of different sub-grids, which could greatly improve communication efficiency. Through linear matrix inequality (LMI) technology and Lyapunov analysis methods, sufficient conditions that guarantee the prescribed H_∞ performance of the studied system are derived. Decentralized controller gains and protocol parameters are obtained simultaneously. The main contributions are summarized as follows.

(1) RR and TOD protocols are used to deal with the multi-node collision of large-scale power systems, which improve communication efficiency greatly. Compared with the existing LFC methods[10,23,24], the scheduling process under multi-area transmission schemes is investigated.

(2) An networked power system impulsive closed-loop model is well constructed, which covers the multi-channel scheduling, packet dropout, disturbance, and network-induced delays in a unified framework. Compared with the system without disturbance[19], this paper studies the anti-disturbance performance of the studied system. An H_∞ LFC method is presented to obtain decentralized controller gains and scheduling protocol parameters simultaneously.

1.1. Notations
Throughout this paper, $\mathbb{R}_n$ stands for the n-dimensional Euclidean space with vector norm $\| \cdot \|$. $diag\{\cdots\}$ and $col\{\cdots\}$ denote the block-diagonal matrix and block-column vector, respectively. The superscript T stands for
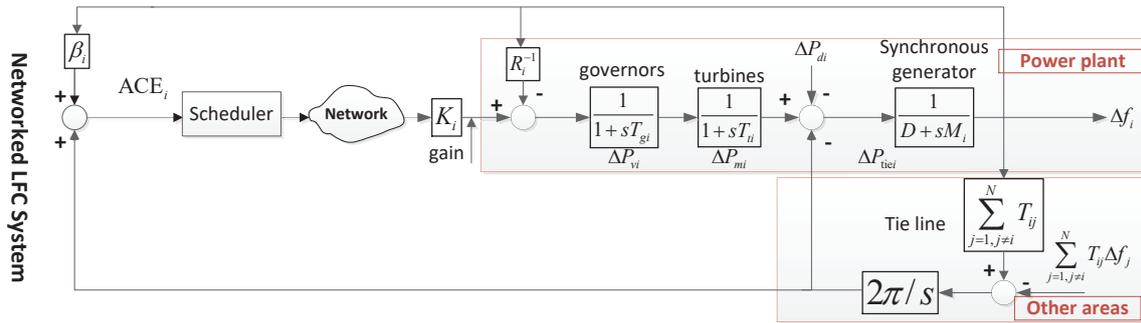
Figure 1. Multi-area decentralized power systems under scheduling protocols.

the transpose of a matrix or a vector. I is an identity matrix with an appropriate dimension. Matrix $X > 0(X \geq 0)$ means that X is a positive definite (positive semi-definite) symmetric matrix. The symbol $*$ is the symmetric term in a matrix. $w[-h, 0]$ denotes the Banach type of absolutely continuous functions $\phi : [-h, 0] \to \mathbb{R}_n$ with $\dot{\phi} \in \mathbb{L}_2(-h, 0)$ with the norm $\| \phi \|_w = \max_{v \in [-h,0]} \| \phi(v) \| + [\int_{-h}^{0} \| \dot{\phi}(v) \|^2 \, ds]^{\frac{1}{2}}$.

2. PROBLEM FORMULATION

Considering single-packet size constraints, the dynamic model of multi-area interconnected power systems with decentralized load frequency controllers is constructed in this section. An impulsive system model under TOD or RR protocol is established.

2.1. Multi-area decentralized LFC model

Diagram of the multi-area decentralized LFC under scheduling protocols is shown in Figure 1, where data transmission from sensors to decentralize controllers is scheduled by RR or TOD scheduling protocol.

The system model is represented as [23,25]:

$$
\begin{cases}
\dot{x}(t) = Ax(t) - Bu(t) + D\omega(t), \\
y(t) = Cx(t),
\end{cases} \tag{1}
$$

where $x(t) \in \mathbb{R}_x$ is the state vector, $y(t) \in \mathbb{R}_{n_y}$ is the measurement and $\omega(t) \in \mathbb{R}_\omega$ is the disturbance, $u(t) \in \mathbb{R}_u$ is the control input vector. The multi-area power systems consist of generators, turbines, and governors, where ΔP_{vi}, ΔP_{mi}, ΔP_{di}, and Δf_i denote the deviation of valve position, generator mechanical output, load, and the frequency of the ith sub-area, respectively. The area control error $ACE_i(s)$ is

$$
ACE_i(s) = \beta_i \Delta f_i(s) + \Delta P_{tie-i}(s). \tag{2}
$$

The state and measured output signals are

$$
x_i^T(t) = [\Delta f_i(t), \Delta P_{tie-i}(t), \Delta P_{mi}, \Delta P_{vi}(t), \int ACE_i(t)]
$$
$$
\omega_i(t) = \Delta P_{di}(t), \; y_i^T(t) = [ACE_i(t), \int ACE_i(t)]
$$

where $x(t) = [x_1^T(t), \cdots, x_n^T(t)]^T$, $y(t) = [y_1^T(t), \cdots, y_n^T(t)]^T \in \mathbb{R}_{n_y}, \omega(t) = [\omega_1^T(t), \cdots, \omega_n^T(t)]^T, A =$

$$[A_{ij}]_{n \times n}, B = diag\{B_1, \cdots, B_n\}, C = [C_1^T, \cdots, C_N^T]^T, F = diag\{F_1, \cdots, F_n\}, C_i = [\underbrace{0, \cdots, 0}_{i-1}, \bar{C}_i, \underbrace{0, \cdots, 0}_{N-i}],$$

$$A_{ii} = \begin{bmatrix} -\frac{D_i}{M_i} & -\frac{1}{M_i} & \frac{1}{M_i} & 0 & 0 \\ 2\pi \sum_{j=1, j \neq i}^{n} T_{ij} & 0 & 0 & 0 & 0 \\ 0 & 0 & -\frac{1}{T_{chi}} & \frac{1}{T_{chi}} & 0 \\ -\frac{1}{R_i T_{gi}} & 0 & 0 & -\frac{1}{T_{gi}} & 0 \\ \beta_i & 1 & 0 & 0 & 0 \end{bmatrix},$$

$$A_{ij} = \begin{bmatrix} 0 & 0 & 0 & 0 & 0 \\ -2\pi T_{ij} & 0 & 0 & 0 & 0 \\ 0 & 0 & 0 & 0 & 0 \\ 0 & 0 & 0 & 0 & 0 \\ 0 & 0 & 0 & 0 & 0 \end{bmatrix}, F_i = \begin{bmatrix} -\frac{1}{M_i} \\ 0 \\ 0 \\ 0 \\ 0 \end{bmatrix}, B_i = \begin{bmatrix} 0 \\ 0 \\ 0 \\ \frac{1}{T_{gi}} \\ 0 \end{bmatrix}, \bar{C}_i^T = \begin{bmatrix} \beta_i & 0 \\ 1 & 0 \\ 0 & 0 \\ 0 & 0 \\ 0 & 0 \end{bmatrix}.$$

The multi-area power system includes N controlled areas, N decentralized controllers, which are connected via the network. Then, measurement signals are given by $y_i(t) = C_i x(t) \in \mathbb{R}_{n_i}, i = 1, \cdots, N, \sum_{i=1}^{N} n_i = n_y$. Based on the phasor measurement unit, sampling instants of N sensors are synchronized in different areas of power systems. Denote sampling instant by s_q, satisfying that $0 = s_0 < s_1 < \cdots < s_q < \cdots, s_{q+1} - s_q \leq \varrho, \lim_{q \to +\infty} s_q = +\infty$, where ϱ is the maximum allowable transfer interval.

In this paper, we take imperfect network conditions into account, such as data loss and network-induced delay. Denote the sequence after packet loss by $\{s_k\} \subseteq \{s_q\}$; that is, only at sampling instants s_k, the input of the controller can be updated. For $i = 1, \cdots, N$, an uncertain, time-varying delay $v_{s_k}^i \in [0, \tau_M^i]$ is assumed to occur, where τ_M^i is delay upper bound of the *ith* channel and $\max_{i=1, \cdots, N} \{\tau_M^i\} = \tau_M$. Buffers are set to store and choose the largest communication delay τ_{s_k} of power system channels, i.e., $\tau_{s_k} = \max_{i=1, \cdots, N} \{v_{s_k}^i\}$. Then, ZOH updating instant is $t_k = s_k + \tau_{s_k}$. The transmission delay is assumed to be bound, satisfying:

$$0 \leq \tau_{s_k} \leq \tau_M, \ t_{k+1} - t_k - \tau_{s_k} \leq \tau_M + \varrho = \bar{\tau}. \tag{3}$$

Let $\hat{y}(s_k) = [\hat{y}_1^T(s_k) \cdots \hat{y}_N^T(s_k)]^T \in \mathbb{R}_{n_y}$ denote the output signal transmitted to the scheduler. At instant s_k, only one node can be active. Let $\iota_k \in \{1, \cdots, N\}$ be the active output node at s_k, which is dependent on the scheduling rule. Then, we have

$$\hat{y}_i(s_k) = \begin{cases} y_i(s_k), i = \iota_k \\ \hat{y}_i(s_{k-1}), i \neq \iota_k \end{cases} \tag{4}$$

Consider the scheduling error between output $y_i(s_k)$ and the last available measurement $\hat{y}_i(s_{k-1})$:

$$e_i(t) = -y_i(s_k) + \hat{y}_i(s_{k-1}), \ e(t) = col\{e_1(t), \cdots, e_N(t)\}, \ t \in [t_k, t_{k+1}), \tag{5}$$

where $\hat{y}_i(s_{-1}) \triangleq 0, i = 1, \cdots, N$. In this paper, controllers and actuators in the *ith* area are event-driven. Let $L_i > 0, i = 1, \cdots, N$ be node weighting matrices. Under TOD scheduling,

$$\iota_k = \arg \max_{i \in \{1, \cdots, N\}} |\sqrt{L_i}(-y_i(s_k) + \hat{y}_i(s_{k-1}))|^2. \tag{6}$$

Under RR scheduling protocol, the active node ι_k is selected periodically:

$$\iota_k = \iota_{k+N}. \tag{7}$$

In the following, we will design the decentralized LFC law under the communication network. Similar to [23], a PI controller is used in this paper:

$$u_i(t) = -K_{Pi}ACE_i(t) - K_{Ii}\int ACE_i(t). \tag{8}$$

Therefore, dynamic model of the scheduled power systems under the decentralized LFC Equation (8) and imperfect network environments can be formalized as

$$\begin{cases} \dot{x}(t) = Ax(t) - BK\hat{y}(s_k) + F\omega(t) \\ y(t) = Cx(t), t \in [t_k, t_{k+1}), \end{cases} \tag{9}$$

where $u(t) = \sum_{i=1}^{N} K_i y_i(t) = Ky(t)$, $K = [K_1, \cdots, K_N]$, $K_i = [K_{Pi}, K_{Ii}]$.

2.2. Impulsive model and study objective

From Equation (5), one can obtain that

$$e_i(t_{k+1}) = \begin{cases} C_i x(s_k) - C_i x(s_{k+1}), i = \iota_k \\ C_i[x(s_k) - x(s_{k+1})] + e_i(t_k), i \neq \iota_k \end{cases} \tag{10}$$

Define an artificial delay $\tau(t) = t - s_k$, from which one arrives at

$$0 \leq \tau_{s_k} \leq \tau(t) \leq s_{k+1} - s_k + \tau_{s_{k+1}} \leq \tau_M, \dot{\tau}(t) = 1. \tag{11}$$

From Equation (5) and Equation (9), the impulsive power system model can be

$$\dot{x}(t) = Ax(t) - BKCx(t - \tau(t)) - \sum_{i=1, i \neq \iota_k}^{N} BK_i C_i e_i(t) + F\omega(t). \tag{12}$$

For system Equation (12), the initial condition of $x(t)$ on $[-\tau_M, 0]$ is supplemented as $x(t) = \phi(t), t \in [-\tau_M, 0]$, with $\phi(0) = x_0$, where $\phi(t)$ is a continuous function on $[-\tau_M, 0]$.

Using scheduling scheme Equation (6) and Equation (7), this paper is to design the decentralized controller Equation (8) such that system Equation (12) is exponentially stable with a prescribed H_∞ performance γ.

3. MAIN RESULTS

In the following, we first derive sufficient criteria under scheduling scheme Equation (6) and Equation (7) to ensure the exponential stability of system Equation (12) with a prescribed H_∞ performance. Then, criteria are proposed to design decentralized controllers under multi-channel transmission.

3.1. Stability analysis under the TOD scheduling scheme Eqution (6)

Construct Lyapunov-Krasovskii functional candidate:

$$V(t) = \sum_{i=1}^{N} e_i^T(t) L_i e_i(t) + \Pi(t) + V_H, \tag{13}$$

where $O > 0, H_i > 0, T > 0, L_i > 0, \alpha > 0, S > 0, i = 1, \cdots, N, t \in [t_k, t_{k+1})$,

$$V_H = \sum_{i=1}^{N} \int_{s_k}^{t} \tau_M e^{2\alpha(s-t)} \left\| \sqrt{H_i} C_i \dot{x}(s) \right\|^2 ds,$$

$$\Pi(t) = \int_{t-\tau_M}^{t} e^{2\alpha(s-t)} x^T(s) Sx(s) ds + x^T(t) Ox(t) + \tau_M \int_{t-\tau_M}^{t} \int_{s}^{t} e^{2\alpha(s-t)} \dot{x}^T(v) T\dot{x}(v) dv ds.$$

Remark 1 V_H is introduced to cope with reset conditions, which is continuous on $[t_k, t_{k+1})$, and does not grow in the jumps when $t = t_{k+1}$ since

$$-V_H(t_{k+1}^-) + V_H(t_{k+1}) \le -\sum_{i=1}^{N} e^{-2\alpha\tau_M} \left\| \sqrt{H_i} C_i(-x(s_{k+1}) + x(s_k)) \right\|^2 \tag{14}$$

Theorem 1 Under TOD scheduling scheme *Equation (6)*, for given scalars $\tau_M, \alpha > 0, \gamma > 0$, impulsive system *Equation (12)* is exponentially stable with a prescribed H_∞ performance γ, if there exist appropriate dimensions Y and real matrices $O > 0, S > 0, T > 0, H_i > 0, J_i > 0, L_i > 0, i = 1, \cdots, N$ such that

$$\begin{bmatrix} \Xi_{11} & * & * \\ \Xi_{21} & \Xi_{22} & * \\ \Xi_{31} & 0 & \Xi_{33} \end{bmatrix} < 0, \tag{15}$$

$$\begin{bmatrix} T & Y^T \\ Y & T \end{bmatrix} > 0, \tag{16}$$

$$\Omega_i = \begin{bmatrix} \Omega_{11} & \Omega_{12} \\ * & \Omega_{22} \end{bmatrix} < 0 \tag{17}$$

are feasible for $i, j = 1, \cdots, N$, where

$$\Xi_{11} = \begin{bmatrix} \Psi_{11} & \Psi_{12} & \Psi_{13} & \Psi_{14} & \Psi_{15} \\ * & \Psi_{22} & \Psi_{23} & 0 & 0 \\ * & * & \Psi_{33} & 0 & 0 \\ * & * & * & \Psi_{44} & 0 \\ * & * & * & * & \Psi_{55} \end{bmatrix}, \bar{\xi}_i = \begin{cases} [-PBK_2C_2, \cdots, -PBK_NC_N], \iota_k = 1 \\ [-PBK_1C_1, \cdots, -PBK_{N-1}C_{N-1}], \iota_k = N \\ [-PBK_1C_1, \cdots, -PBK_jC_{j|j\neq\iota_k}, \cdots, -PBK_NC_N], \iota_k \neq 1, N \end{cases}$$

$$\phi_i = \begin{cases} diag\{\psi_2, \cdots, \psi_N\}, \iota_k = 1 \\ diag\{\psi_1, \cdots, \psi_{N-1}\}, \iota_k = N \\ diag\{\psi_1, \cdots, \psi_{j|j\neq\iota_k}, \cdots, \psi_N\}, \iota_k \neq 1, N \end{cases}, \pi_i = \begin{cases} [BK_2C_2, \cdots, BK_NC_N], \iota_k = 1 \\ [BK_1C_1, \cdots, BK_{N-1}C_{N-1}], \iota_k = N \\ [BK_1C_1, \cdots, BK_jC_{j|j\neq\iota_k}, \cdots, BK_NC_N], \iota_k \neq 1, N. \end{cases}$$

$$\Psi_{11} = OA + A^T O + 2\alpha O + S + T, \Psi_{13} = -Y^T, \Psi_{14} = \chi_i, \Psi_{23} = Y^T - T, F_i = [A, BKC, 0, \pi_i, F],$$

$$\Psi_{22} = 2T - Y - Y^T, \Psi_{33} = T - S, \Psi_{44} = \chi_i, \Omega_{11} = -\frac{1-2\alpha\tau_M}{N-1} L_i + J_i, \Psi_{12} = -OBKC - T + Y^T,$$

$$\chi_i = [-OBK_1C_1, \cdots, -OBK_NC_N], \Omega_{22} = L_i - H_i e^{-2\alpha\tau_M}, \Xi_{22} = diag\{-T, -H_1, \cdots, -H_N\},$$

$$\Psi_{15} = OF, \Omega_{12} = L_i, \Xi_{21} = [\tau_M T F_i, \sqrt{\tau_M} H_1 C_1 F_1, \cdots, \sqrt{\tau_M} H_N C_N F_N], \Psi_{55} = -\gamma^2 I,$$

$$\psi_j = -\frac{1}{\tau_M} J_j + 2\alpha L_j, \Theta = \tau_M^2 T + \tau_M \sum_{i=1}^{N} C_i^T H_i C_i, \Xi_{31} = [C, 0, \cdots, 0].$$

Proof: Differentiating $V(t)$ along *Equation (12)* and applying Wirtinger-based integral inequality [26], we can obtain

$$\dot{V}(t) + 2\alpha V(t) - \frac{1}{\tau_M} \sum_{i=1, i\neq\iota_k}^{N} |\sqrt{J_i} C_i e_i(t)|^2 - 2\alpha |\sqrt{L_{\iota_k}} e_{\iota_k}(t)|^2 + |y(t)|^2 - \gamma^2 |\omega(t)|^2 \le -\frac{1}{\tau_M} \sum_{l=1, l\neq i}^{N} |\sqrt{J_l} C_l e_l(t)|^2$$

$$-\gamma^2 |\omega(t)|^2 - e^{-2\alpha\tau_M} x^T(t - \tau_M) S x(t - \tau_M) + |y(t)|^2 + \dot{x}^T(t) \Theta \dot{x}(t) - e^{-2\alpha\tau_M} \tau_M \int_{t-\tau_M}^{t} \dot{x}^T(s) T \dot{x}(s) ds \tag{18}$$

$$+ 2\alpha \sum_{l=1, l\neq i}^{N} e_l^T(t) C_l L_l C_l e_l(t) + 2x^T(t) O \dot{x}(t) + x^T(t)(2\alpha O + S) x(t),$$

where $\xi_i(t) = col\{x(t), x(t - \tau(t)), x(t - \tau_M), \bar{\xi}_i(t), \omega(t)\}$.

We use the reciprocally convex approach [27] to deal with the cross item in Equation (18). By using Schur's complement, one can get

$$\dot{V}(t) + 2\alpha V(t) - \frac{1}{\tau_M} \sum_{i=1, i \neq \iota_k}^{N} |\sqrt{J_i} C_i e_i(t)|^2 - 2\alpha |\sqrt{L_{\iota_k}} e_{\iota_k}(t)|^2 + |y(t)|^2 - \gamma^2 |\omega(t)|^2 < 0. \tag{19}$$

In the following, we will prove that

(i) with $\omega(t) = 0$, the impulsive system Equation (12) is exponentially stable.

Since $\frac{d}{dt} e^{2\alpha t} V(t) = e^{2\alpha t} (\dot{V}(t) + 2\alpha V(t))$ and $V(t)$ is continuous in $t \in [t_k, t_{k+1})$, the integration of Equation (19) yields

$$e^{2\alpha t} V(t) - e^{2\alpha t_k} V(t_k) \leq \int_{t_k}^{t} e^{2\alpha s} ds [2\alpha |\sqrt{L_{\iota_k}} e_{\iota_k}(t)|^2 + \frac{1}{\tau_M} \sum_{i=1, i \neq \iota_k}^{N} |\sqrt{J_i} C_i e_i(t)|^2]. \tag{20}$$

It follows from $\int_{t_k}^{t} e^{2\alpha(s-t)} ds \leq \tau_M$ that

$$V(t_{k+1}) \leq \Theta_k + e^{2\alpha(t_k - t_{k+1})} V(t_k), \tag{21}$$

where

$$\Theta_k = \sum_{j=1}^{N} [-V_H(t_{k+1}^-) + |\sqrt{L_{\iota_k}} e_{\iota_k}(t_{k+1})|^2 - |\sqrt{L_{\iota_k}} e_{\iota_k}(t_k)|^2 + V_H(t_{k+1})] + \sum_{i=1, i \neq \iota_k}^{N} |\sqrt{J_i} C_i e_i(t)|^2 + 2\alpha \tau_M |\sqrt{L_{\iota_k}} e_{\iota_k}(t_k)|^2. \tag{22}$$

Then taking Equation (17) and Equation (22) into account, denoting $\kappa_i = [e_i(t_k), C_i[-x(s_{k+1}) + x(s_k)]]^T$, we have

$$\Theta_k \leq -|(\sqrt{H_{\iota_k}} e^{-2\alpha \tau_M} - \sqrt{L_{\iota_k}}) C_{\iota_k} [x(s_k) - x(s_{k+1})]|^2 + \sum_{i=1, i \neq \iota_k}^{N} \kappa_i \Omega_i \kappa_i \leq 0. \tag{23}$$

Hence, one can conclude that

$$V(t) \leq \sum_{i=1, i \neq \iota_k}^{N} |\sqrt{J_i} e_i(t_k)|^2 + e^{2\alpha(t_0 - t)} V(t_0) + 2\alpha \tau_M |\sqrt{L_{\iota_k}} e_{\iota_k}(t_k)|^2. \tag{24}$$

From Equation (24), we have

$$V(t) \geq \lambda_{min}\{O\} |x(t)|^2 + \sum_{i=1}^{N} |\sqrt{L_i} e_i(t)|^2,$$

which implies that

$$\lambda_{min}\{O\} |x(t)|^2 \leq (2\alpha \tau_M - 1) |\sqrt{L_{\iota_k}} e_{\iota_k}(t)|^2 + \sum_{i=1, i \neq \iota_k}^{N} |\sqrt{J_i - L_i} e_i(t)|^2 + e^{2\alpha(t_0 - t)} V(t_0).$$

It follows from $\Omega_i < 0$ that for $t \geq t_0$

$$\lambda_{min}\{O\} |x(t)|^2 \leq e^{2\alpha(t_0 - t)} V(t_0). \tag{25}$$

For $t < t_0$, the system takes the form $\dot{x} = Ax(t) + F\omega(t)$, then its corresponding solution is given by

$$x(t) = e^{At} x(0) + \int_0^t e^{A(-s+t)} F\omega(s) ds. \tag{26}$$

Clearly, there exists the maximum of $|x(t)|$ for $t \in [t_0 - \tau_M, t_0]$. Thus, $V(t_0) \leq \mu \|x_{t_0}\|_W^2 + \sum_{i=1}^N e_i^T(t_0) L_i e_i(t_0)$ for some $\mu > 0$.

Therefore, the exponential stability of the system Equation (12) with $\omega(t) = 0$ is guaranteed.

Next, we will show that

(ii) under the zero initial condition, the inequality $\|y\|_{L_2} \leq \gamma \|\omega\|_{L_2}$ holds for any nonzero $\omega \in L_2[0, +\infty)$.

From Equation (19), we obtain that for $t \in [t_k, t_{k+1})$,

$$|y(t)|^2 - \gamma^2 |\omega(t)|^2 \leq -\dot{V}(t) + 2\alpha |\sqrt{L_{\iota_k}} e_{\iota_k}(t)|^2 + \frac{1}{\tau_M} \sum_{i=1, i \neq \iota_k}^N |\sqrt{J_i} C_i e_i(t)|^2. \tag{27}$$

Integrating Equation (27) on t from t_k to t_{k+1}^- yields

$$\int_{t_k}^{t_{k+1}^-} |y(s)|^2 - \gamma^2 |\omega(s)|^2 ds + V(t_{k+1}) \leq V(t_k) + \Theta_k \leq V(t_k). \tag{28}$$

Then, by summing Equation (28) on k from 0 to ρ, where $\rho \to +\infty$, we have

$$\int_{t_0}^{t_{\rho+1}^-} (|y(s)|^2 - \gamma^2 |\omega(s)|^2) ds \leq V(t_0). \tag{29}$$

Under the zero initial condition, $\int_0^{+\infty} y^T(s) y(s) ds \leq \int_0^{+\infty} \gamma^2 \omega^T(s) \omega(s) ds$. Therefore, one can derive that under the zero initial condition, $\|y\|_{L_2} \leq \gamma \|\omega\|_{L_2}$ for any nonzero $\omega \in L_2[0, +\infty)$. This completes the proof. □

Remark 2 *The feasibility of the linear martix inequalities has been sufficiently explained in*[23,28]. *Due to page limitations, this part is omitted here.*

3.2. Stability analysis under the RR scheduling scheme Eqution (7)
Construct the following Lyapunov-Krasovskii functional candidate:

$$V(t) = \Pi(t) + V_H + V_L, \ k \geq N - 1, \ t \in [t_k, t_{k+1}), \tag{30}$$

where

$$V_H = \begin{cases} \sum_{i=1}^{N-1} \tau_M \int_{s_k}^t e^{2\alpha(s-t)} |\sqrt{H_i} C_i \dot{x}(s)| ds, \ k \neq N-1, \\ \sum_{i=1}^{N-1} \tau_M \int_{s_0}^t e^{2\alpha(s-t)} |\sqrt{H_i} C_i \dot{x}(s)| ds, \ k = N-1, \end{cases}$$

$$H_i = (N-1) L_i e^{2\alpha(N-1)\tau_M}, V_L = \sum_{i=1}^{N-1} \frac{t_{k+1} - t}{i \tau_M} |\sqrt{L_{\iota_{k-j}}} e_{\iota_{k-j}}(t)|^2.$$

Similar to Theorem 5.2 in[29], we establish the following result.

Theorem 2 *Under RR scheduling scheme Equation (7), given $\tau_M > 0$ and $\alpha > 0$, assume that there exist matrices $O > 0, S > 0, T > 0, L_i > 0, i = 1, \cdots, N$ and Y with appropriate dimensions such that Equation (15) and Equation (16) are feasible with $J_i = \frac{L_i}{N-1}$, where G_i is given by Equation (30). Then, system Equation (12) is exponentially stable with a prescribed H_∞ performance γ.*

Proof: The detailed derivation process can refer to[29] and the proof of Theorem 1, which is omitted here due to the limited pages. □

3.3. Controller Design under the TOD scheduling scheme Equation (6)

Theorem 3 *Under TOD scheduling scheme Equation (6), for given matrices A, B, C, F, and scalars $\tau_M, \alpha > 0, \gamma > 0, \zeta > 0$, system Equation (12) is exponentially stable with a prescribed H_∞ performance γ, if there exist real matrices $Z > 0, \tilde{S} > 0, \tilde{T} > 0, i, j = 1, \cdots, N, \tilde{J}_i > 0, H_i > 0, \tilde{L}_i > 0$ and appropriate dimensions $\tilde{Y}, \beth, \digamma$ such that*

$$min\ tr\left\{\sum_{i=1}^{N} H_i h_i\right\} \tag{31}$$

s.t. Equation (17), Equation (32)*, Equation (33), Equation (34), Equation (35)

$$\begin{bmatrix} \tilde{\Xi}_{11} & * & * \\ \tilde{\Xi}_{21} & \tilde{\Xi}_{22} & * \\ \tilde{\Xi}_{31} & 0 & \tilde{\Xi}_{33} \end{bmatrix} < 0, \tag{32}$$

$$\begin{bmatrix} \tilde{T} & \tilde{Y}^T \\ \tilde{Y} & \tilde{T} \end{bmatrix} > 0, \tag{33}$$

$$\begin{bmatrix} h_i & * \\ I & H_i \end{bmatrix} > 0, \tag{34}$$

$$\begin{bmatrix} -\zeta I & (\beth C - CZ)^T \\ \beth C - CZ & -I \end{bmatrix} < 0, \tag{35}$$

is solvable, and the controller gain is given by $K = \digamma\beth^{-1}$, where Equation (32)* is equivalent to Equation (32) by replacing $-H_i^{-1} - Z^T \tilde{T}_r^{-1} Z$ with $-h_i, \rho^2 \tilde{T}_r - 2\rho Z$, and

$$\tilde{\Xi}_{11} = \begin{bmatrix} \tilde{\Psi}_{11} & \tilde{\Psi}_{12} & \tilde{\Psi}_{13} & \tilde{\Psi}_{14} & \tilde{\Psi}_{15} \\ * & \tilde{\Psi}_{22} & \tilde{\Psi}_{23} & 0 & 0 \\ * & * & \tilde{\Psi}_{33} & 0 & 0 \\ * & * & * & \tilde{\Psi}_{44} & 0 \\ * & * & * & * & \tilde{\Psi}_{55} \end{bmatrix},$$

$$\tilde{\phi}_i = \begin{cases} diag\{\tilde{\psi}_2, \cdots, \tilde{\psi}_N\}, \iota_k = 1 \\ diag\{\tilde{\psi}_1, \cdots, \tilde{\psi}_{N-1}\}, \iota_k = N \\ diag\{\tilde{\psi}_1, \cdots, \tilde{\psi}_{j|j\neq \iota_k}, \cdots, \tilde{\psi}_N\}, \iota_k \neq 1, N \end{cases}$$

$$\tilde{\bar{\xi}}_i = \begin{cases} [-BK_2 C_2 Z, \cdots, -BK_N C_N Z], \iota_k = 1 \\ [-BK_1 C_1 Z, \cdots, -BK_{N-1} C_{N-1} Z], \iota_k = N \\ [-BK_1 C_1 Z, \cdots, -BK_j C_{j|j\neq \iota_k} Z, \cdots, -BK_N C_N Z], \iota_k \neq 1, N \end{cases}$$

$\tilde{\psi}_j = -\frac{1}{\tau_M} \tilde{J}_j + 2\alpha \tilde{L}_j, \tilde{\Xi}_{33} = -I, \tilde{\Psi}_{11} = AZ + ZA^T + 2\alpha Z + \tilde{S} + \tilde{T}, \tilde{\Psi}_{12} = -BKCZ - \tilde{T} + \tilde{Y}^T, \tilde{\Psi}_{22} = 2\tilde{T} - \tilde{Y} - \tilde{Y}^T, \tilde{T} = ZTZ,$

$\tilde{\Psi}_{23} = \tilde{Y}^T - \tilde{T}, \tilde{\chi}_i = [-BK_1 C_1 Z, \cdots, -BK_N C_N Z], \tilde{\Psi}_{33} = \tilde{T} - \tilde{S}, \tilde{\Psi}_{14} = \tilde{\chi}_i, \tilde{\Psi}_{44} = \tilde{\phi}_i, \tilde{\Psi}_{55} = -\gamma^2 I, \tilde{\Psi}_{13} = -\tilde{Y}^T, \tilde{S} = ZSZ,$

$\tilde{\Xi}_{31} = [CZ, 0, \cdots, 0], \tilde{\Xi}_{22} = diag\{-Z\tilde{T}^{-1}Z, -H_1^{-1}, \cdots, -H_N^{-1}\}, \tilde{\Xi}_{21}^T = [\tau_M F_i, \sqrt{\tau_M} C_1 F_1, \cdots, \sqrt{\tau_M} C_N F_N], \tilde{Y} = ZYZ.$

Proof: Let $Z = O^{-1}, \tilde{J}_i = ZJ_i Z, \tilde{L}_i = ZL_i Z, i = 1, \cdots, N$. Pre- and post-multiplying Equation (15) and Equation (16) with

$$diag\{Z, \cdots, Z, I, T^{-1}, H_1^{-1}, \cdots, H_N^{-1}, I, Z\}$$

Table 1. Configuration of three-area power systems

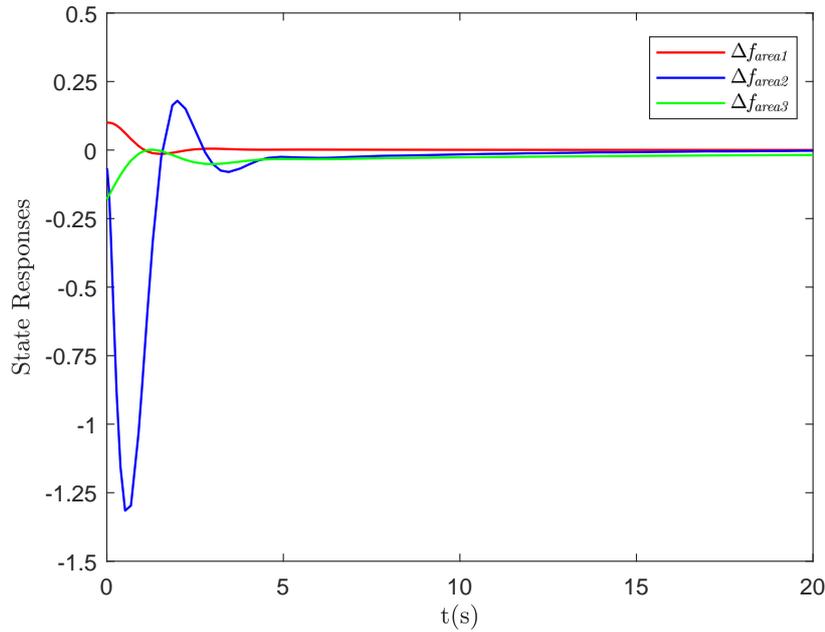| Parameter	$T_{ch}(s)$	$T_g(s)$	R	D	β	$M(s)$
Area1	0.30	0.37	0.05	1.0	$\frac{1}{R_1}+D_1$	10
Area2	0.17	0.40	0.05	1.5	$\frac{4}{R_2}+D_2$	10
Area3	0.20	0.35	0.05	1.8	$\frac{5}{R_3}+D_3$	12
$T_{12}=0.20, T_{13}=0.12, T_{23}=0.25(pu/rad)$						

Figure 2. State responses of case 1.

and their transposes, respectively. For the nonlinear terms $-Z\tilde{T}_r^{-1}Z, r = 1, 2$ and $-H_i^{-1}$, using inequalities $-Z\tilde{T}_r^{-1}Z \leq \rho^2\tilde{T}_r - 2\rho Z$ and the cone complementary linearization algorithm in [27], one can obtain *Equation* (32)*. By solving the minimization problem Equation (31), system Equation (12) is exponentially stable with a prescribed H_∞ performance γ and $K = F\beth^{-1}$. □

3.4. Controller design under the RR scheduling scheme Equation (7)
Similar to Theorem 5.2 in [29], we establish Theorem 4.

Theorem 4 *Under the RR scheduling scheme Equation (7), for given matrices A, B, C, F, and scalars $\tau_M, \alpha > 0, \gamma > 0, \zeta > 0$, system Equation (12) is exponentially stable with a prescribed H_∞ performance γ, if there exist real matrices $Z > 0, \tilde{S} > 0, \tilde{T} > 0, \tilde{L}_i > 0, i = 1, \cdots, N$ and $\tilde{Y}, \beth, F$ with appropriate dimensions such that Equation (31) is solvable with $J_i = \frac{L_i}{N-1}$, where H_i is given by Equation (30). The controller gain is given by $K = F\beth^{-1}$.*

Proof: The detailed derivation process can refer to [29] and the proof of Theorem 3, which is omitted here. □

4. AN ILLUSTRATIVE EXAMPLE

In the following, we use a three-area power system [23,24,28] interconnected by the shared communication network to demonstrate the effectiveness of main results. Parameters are listed in Table 1.

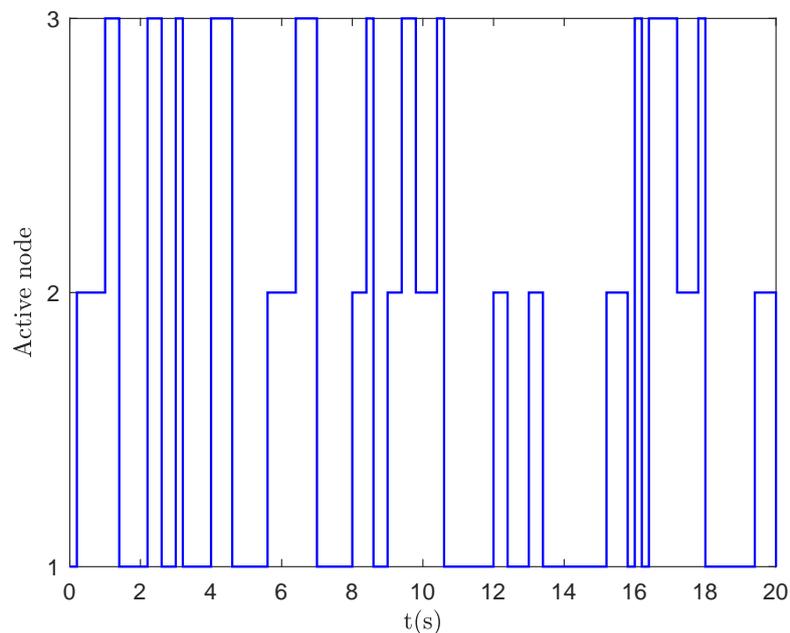**Case 1:** Stability of the studied system under TOD scheduling scheme Equation (6) and $\omega(t) = 0$.

Figure 3. The switching behavior of active nodes of case 1.

Assume parameters are chosen as $\tau_M = 0.1s, \gamma = 10, \rho = 0.63$. We apply Theorem 3 which yields $K_1 = [0.2393, 0.0224]$, $K_2 = [0.2379, -0.1352]$, $K_3 = [0.2324, 0.1965]$.

Correspondingly, state responses and the switching behavior of active nodes are illustrated by Figure 2 and 3, respectively. Clearly, the designed dynamics output feedback controllers can stabilize the three-area power system under the TOD scheduling scheme Equation (6) in the absence of disturbance.

Case 2: Stability of the studied system under RR scheduling scheme Equation (7) and $\omega(t) = 0$.

To compare with the TOD protocol Equation (6), we use the same parameters as case 1. We apply Theorem 4 which yields $K_1 = [0.1876, 0.0184]$, $K_2 = [0.1899, -0.1596]$, $K_3 = [0.1824, 0.1498]$. Then, state responses and the switching behavior of active nodes are depicted in Figure 4 and 5. From Figure 2-5, one can obtain that the system can be stable under both scheduling protocols Equation (6), Equation (7). Compared with RR protocol, TOD protocol can achieve dynamic scheduling, which makes the control process more efficient.

Case 3: Stability of the studied system under TOD scheduling scheme Equation (6) and $\omega(t) \neq 0$.

According to Theorem 1-4, TOD protocol can degrade into RR protocol under certain conditions. In this case, we take the TOD protocol Equation (6) as an example to verify the anti-disturbance performance of the studied system. Under the disturbance $\omega(t)$ shown in Figure 6, we obtain controller gains $K_1 = [0.4005, -0.1702]$, $K_2 = [0.4839, -0.2094]$, $K_3 = [0.4914, -0.4009]$. State responses of the system are depicted in Figure 7. The designed decentralized controllers under the TOD protocol Equation (6) can ensure system stability with load disturbances.
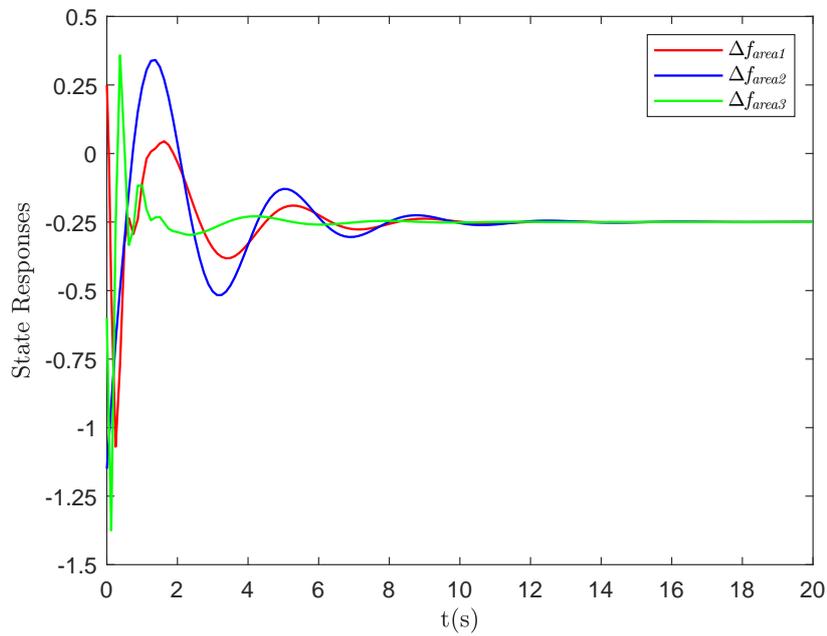
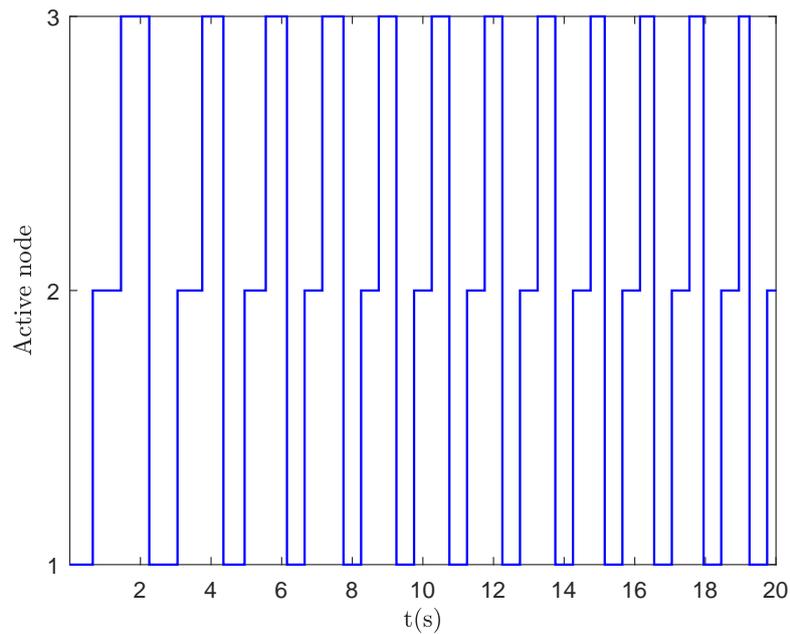**Figure 4.** State responses of case 2.

Figure 5. The switching behavior of active nodes of case 2.

5. CONCLUSIONS

This paper has designed H_∞ output feedback decentralized load frequency controllers for multi-area power systems under the shared but band-limited network. TOD and RR protocols have been used to improve communication efficiency. Since transmission priority has been well designed under scheduling protocols, a higher control performance has been obtained. Then, decentralized output feedback controllers with the prescribed
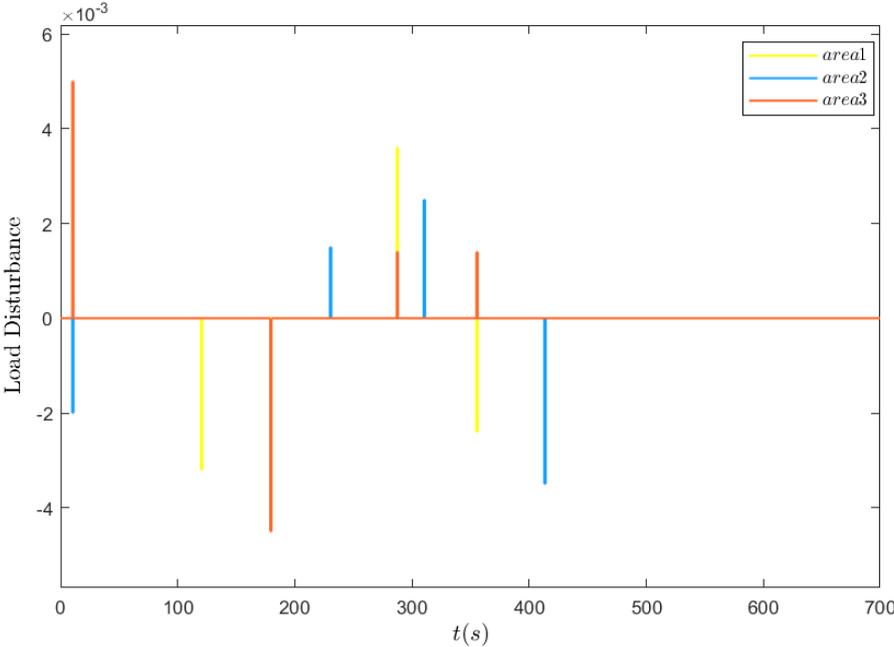
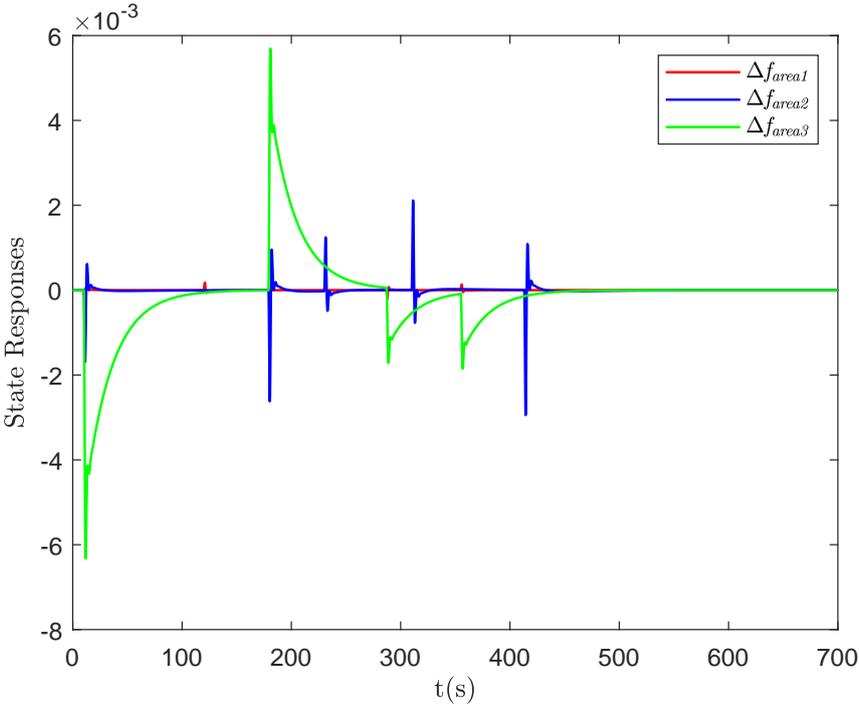**Figure 6.** Disturbance of case 3.

Figure 7. State responses of case 3.

performance have been designed in different areas. Finally, an example has verified the effectiveness of main results.

DECLARATIONS

Authors' contributions
Made substantial contributions to the research, idea generation, algorithm design, performed critical review, commentary and revision, as well as provided administrative, technical, and material support: Peng C
Conceived and designed the experiments, analyzed simulation results, wrote and edited the original draft: Yang H

Availability of data and materials
Not applicable.

Conflicts of interest
All authors declared that there are no conflicts of interest.

Ethical approval and consent to participate
Not applicable.

Consent for publication
Not applicable.

REFERENCES

1. Mohandes B, El Moursi MS, Hatziargyriou N, El Khatib S. A review of power system flexibility with high penetration of renewables. *IEEE Trans Power Syst* 2019;34:3140–55. DOI
2. Ranjan M, Shankar R. A literature survey on load frequency control considering renewable energy integration in power system: Recent trends and future prospects. *J Energy Stor* 2022;45:103717. DOI
3. Peng C, Li F. A survey on recent advances in event-triggered communication and control. *Inform Sci* 2018;457:113–25. DOI
4. Zhou Q, Shahidehpour M, Paaso A, et al. Distributed control and communication strategies in networked microgrids. *IEEE Communic Surv & Tutori* 2020;22:2586–633. DOI
5. Shang Y. Group consensus of multi-agent systems in directed networks with noises and time delays. *Int J Syst Sci* 2015;46:2481–92. DOI
6. Alhelou HH, Hamedani-Golshan ME, Zamani R, Heydarian-Forushani E, Siano P. Challenges and opportunities of load frequency control in conventional, modern and future smart power systems: a comprehensive review. *Energies* 2018;11:2497. DOI
7. Yan Z, Xu Y. Data-driven load frequency control for stochastic power systems: a deep reinforcement learning method with continuous action search. *IEEE Trans Power Syst* 2018;34:1653–56. DOI
8. Peng C, Wu J, Tian E. Stochastic event-triggered H_∞ control for networked systems under denial of service attacks. *IEEE Trans Syst, Man, Cybern: Systems* 2021. DOI
9. Shangguan XC, He Y, Zhang CK, et al. Control performance standards-oriented event-triggered load frequency control for power systems under limited communication bandwidth. *IEEE Trans Contr Syst Technol* 2021;30:860–68. DOI
10. Tian E, Peng C. Memory-based event-triggering H_∞ load frequency control for power systems under deception attacks. *IEEE Trans Cybern* 2020;50:4610–18. DOI
11. Peng C, Sun H, Yang M, Wang YL. A survey on security communication and control for smart grids under malicious cyber attacks. *IEEE Trans Syst, Man, Cybern: Systems* 2019;49:1554–69. DOI
12. Wang D, Chen F, Meng B, Hu X, Wang J. Event-based secure H_∞ load frequency control for delayed power systems subject to deception attacks. *Appl Mathem Comput* 2021;394:125788. DOI
13. Wu J, Peng C, Yang H, Wang YL. Recent advances in event-triggered security control of networked systems: a survey. *Int J Syst Sci* 2022;0:1–20. DOI
14. Freirich D, Fridman E. Decentralized networked control of systems with local networks: a time-delay approach. *Automatica* 2016;69:201–9. DOI

15. Liu K, Fridman E, Hetel L, Richard JP. Sampled-data stabilization via round-robin scheduling: a direct Lyapunov-Krasovskii approach. *IFAC Proceed Vol* 2011;44:1459–64. DOI

16. Ding D, Wang Z, Han QL, Wei G. Neural-network-based output-feedback control under round-robin scheduling protocols. *IEEE trans cybern* 2018;49:2372–84. DOI

17. Zou L, Wang Z, Han QL, Zhou D. Full information estimation for time-varying systems subject to Round-Robin scheduling: A recursive filter approach. *IEEE Trans Syst, Man, Cybern: Systems* 2019;51:1904–16. DOI

18. Zhang XM, Han QL, Ge X, et al. Networked control systems: a survey of trends and techniques. *IEEE/CAA J Autom Sinica* 2019;7:1–17. DOI

19. Liu K, Fridman E, Hetel L. Network-based control via a novel analysis of hybrid systems with time-varying delays. In: *2012 IEEE 51st IEEE Confer Decis Contr (CDC)*. IEEE; 2012. pp. 3886–91. DOI

20. Zhang J, Peng C, Xie X, Yue D. Output feedback stabilization of networked control systems under a stochastic scheduling protocol. *IEEE trans cybern* 2019;50:2851–60. DOI

21. Liu K, Fridman E, Johansson KH. Networked control with stochastic scheduling. *IEEE Trans Autom Contr* 2015;60:3071–76. DOI

22. Zhang J, Peng C. Networked H_∞ filtering under a weighted TOD protocol. *Automatica* 2019;107:333–41. DOI

23. Peng C, Zhang J, Yan H. Adaptive event-triggering H_∞ load frequency control for network-based power systems. *IEEE Trans Industr Electr* 2017;65:1685–94. DOI

24. Sun H, Peng C, Yue D, Wang YL, Zhang T. Resilient load frequency control of cyber-physical power systems under QoS-dependent event-triggered communication. *IEEE Trans Syst, Man, Cybernet: Systems* 2020;51:2113–22. DOI

25. Shang Y. Median-based resilient consensus over time-varying random networks. *IEEE Trans Circ Syst II: Express Briefs* 2021;69:1203–7. DOI

26. Seuret A, Gouaisbaut F. Wirtinger-based integral inequality: application to time-delay systems. *Automatica* 2013;49:2860–66. DOI

27. El Ghaoui L, Oustry F, AitRami M. A cone complementarity linearization algorithm for static output-feedback and related problems. *IEEE trans autom contr* 1997;42:1171–76. DOI

28. Peng C, Li J, Fei M. Resilient Event-Triggering H_∞ load frequency control for multi-area power systems with energy-limited DoS attacks. *IEEE Trans Power Syst* 2016;32:4110–18. DOI

29. Liu K, Fridman E, Xia Y. Networked control under communication constraints. Springer; 2020.